Widely Tunable, Narrow-Linewidth, High-Peak-Power, Picosecond Midinfrared Optical Parametric Amplifier

Qiang Fu, Lin Xu, Sijing Liang, David P. Shepherd, David J. Richardson, and Shaif-ul Alam

***Abstract*—We report a widely tunable, narrow-linewidth, mid-infrared cascaded optical parametric generator–optical parametric amplifier (OPG–OPA) based on orientation-patterned GaAs pumped by a 46-ps, 1-MHz, 1952-nm diode-seeded thulium(Tm) doped fiber master oscillator power amplifier (MOPA). The Tm-doped-fiber MOPA beam was split by a polarizing beam splitter into two arms to pump the OPG and OPA stages, respectively. The generated signal from the OPG was spectrally filtered by a diffraction grating combined with an adjustable aperture to act as the tunable seed light for the OPA. Widely tunable output in the range of 2552–2960 nm (signal) and 5733–8305 nm (idler) was obtained from the OPA with narrow linewidths of 1.4 cm^{-1} (signal, 2942 nm) and 9 cm^{-1} (idler, 5800 nm), respectively. The maximum pulse energy of 0.40 μJ (signal, 2942 nm) and 0.16 μJ (idler, 5800 nm) was obtained at an overall conversion efficiency of 22.4% for the OPA stage. The pulse duration of the generated signal was 36 ps and assuming the generated idler had the same pulse duration the corresponding maximum peak powers were calculated to be 11.1 kW (signal) and 4.5 kW (idler), respectively.**

***Index Terms*—Mid-infrared lasers, nonlinear optics, optical parametric generator, optical parametric amplifier, orientation-patterned GaAs, quasi phase-matching.**

I. Introduction

MID-INFRARED (mid-IR, 2 to 20 μm) laser sources play an important role in molecular spectroscopy and chemical sensing because organic molecules can be identified through their complex and distinguishable absorption spectra in this spectral region [1]–[5]. However, only a few laser sources can directly generate coherent light in the mid-IR. Of these, quantum cascade lasers, interband cascade lasers and lead-salt diode lasers have received much attention, being robust, compact, and easy to handle [1], [6]–[9], but their relatively low output power and narrow tuning range still limit their applications.

Manuscript received November 17, 2017; revised December 23, 2017; accepted December 29, 2017. Date of publication January 8, 2018; date of current version January 25, 2018. This work was supported by the Engineering and Physical Sciences Research Council under the Airguide Photonics Programme Grant (EP/P030181/1). The work of Q. Fu was supported by the China Scholarship Council. *(Corresponding author: Lin Xu.)*

The authors are with the Optoelectronics Research Centre, University of Southampton, Southampton SO17 1BJ, U.K. (e-mail: Q.Fu@soton.ac.uk; L.Xu@soton.ac.uk; sl13g14@soton.ac.uk; dps@orc.soton.ac.uk; djr@orc.soton.ac.uk; sua@orc.soton.ac.uk).

Color versions of one or more of the figures in this paper are available online at http://ieeexplore.ieee.org.

Digital Object Identifier 10.1109/JSTQE.2018.2789878

On the other hand, mid-IR optical parametric oscillators (OPOs) and amplifiers (OPAs), using efficient nonlinear frequency conversion, offer high output power and very wide tuning possibilities at the cost of somewhat increased complexity, and have found valuable applications in spectroscopic science [10]–[14]. For mid-IR OPOs, there are several high-performance nonlinear crystals: $ZnGeP_2$ (ZGP) [15], [16], $CdSiP_2$ (CSP) [17], [18], orientation-patterned gallium arsenide (OP-GaAs) [19]–[23], and orientation-patterned gallium phosphide (OP-GaP) [24]–[26]. ZGP and CSP are birefringent crystals with tuning ranges limited by the requirements of birefringent phase-matching. In contrast, OP-GaAs and OP-GaP rely on quasi-phase-matching (QPM), which greatly broadens the potential OPO tuning range in the mid-IR and even far-infrared regions, limited only by the transparency of the nonlinear semiconductor media. In particular, OP-GaAs, with the highest nonlinear gain among all QPM materials, offers a range of attractive properties for mid-IR OPOs and OPAs, including wide transparency (0.9 to 17 μm), high nonlinearity, commercial availability at high quality, and the capability of designer QPM [19], [20], [27], [28]. OP-GaAs has produced good conversion efficiencies and high-level output powers in temporal regimes ranging from continuous wave to femtosecond [20], [23], [29]–[31].

Also in many spectroscopic applications, to achieve high spectral resolution, the mid-IR laser sources employed should not only have wide tunablity but also narrow-linewidth [32]–[35]. To realize narrow-linewidth output, optical spectral-narrowing components such as etalons and diffraction gratings can be placed inside the OPO cavity [36]–[38]. Vodopyanov *et al.* reported a grating tunable 4–14 μm narrow-linewidth (between 2 and 6 cm^{-1}) OP-GaAs OPO, but with a rather complex pump consisting of a 3-μm periodically poled lithium niobate OPO [39]. Dual-cavity doubly-resonant OPOs offer an alternative route to achieve the narrow-linewidth output [40], [41]. Clément *et al.* demonstrated a stable nested-cavity doubly-resonant OP-GaAs OPO generating single-frequency, but with a limited tuning range of 10.3–10.9 μm [41]. Furthermore, OPOs injection-seeded by external narrow-linewidth laser sources can also have reduced spectral bandwidth output, however, the tuning range is restricted by the seed laser [42], [43].

Compared to OPOs, which have relatively complicated cavities and critical alignment restrictions, OPAs with a simple single-pass nature and the possibility of high-power operation have attracted great interest. Generally, OPAs require an

external laser source (normally narrow-linewidth) to serve as the seed for the parametric amplification. In the mid-IR wavelength regime, QCLs have been considered to be a promising seed laser for narrow-linewidth OPAs [44]–[46]. Based on OP-GaAs, Bloom *et al.* reported a 4.5-μm-wavelength QCL seeding a narrow-linewidth OPA pumped by a 2-μm Ho:YAG Q-switched laser. However, the generated wavelength was not tunable due to the wavelength-fixed seed laser [44]. In a later report, Gutty *et al.* demonstrated an OP-GaAs OPA with a wavelength-tunable QCL seed generating 8–10 μm output with narrow-linewidth (<3.5 cm^{-1}), however, the peak power was only 140 W [46]. Recently, our group demonstrated a high-peak-power (13 kW) Cr:ZnSe-laser-seeded tunable OP-GaAs OPA with a tuning range of 2557–2684 nm (signal) and 7168 to 8267 nm (idler) and linewidths of 0.7 cm^{-1} (signal) and 1.4 cm^{-1} (idler) [47]. However, the tunability was again limited by the external seed laser, and the OPA could not fully exploit the spectral range that the OP-GaAs crystal provides.

In this paper, to overcome this problem, we report the development of a widely tunable, narrow-linewidth, mid-IR source based on a cascaded OP-GaAs OPG-OPA. A diffraction grating together with an adjustable aperture is used as a spectral filter to narrow the signal linewidth of the OPG stage, which is then used as the seed for the OPA stage. Tuning ranges of 2552–2960 nm (signal) and 5733–8305 nm (idler) covering the entire wavelength regime that the QPM OP-GaAs provided were demonstrated, and the output signal linewidth was narrowed from 46 cm^{-1} (OPG signal) and 51 cm^{-1} (OPG idler) to 1.4 cm^{-1} (OPA signal) and 9 cm^{-1} (OPA idler), respectively. The maximum signal and idler output powers were 400 mW (signal, 2942 nm) and 162 mW (idler, 5800 nm) with an overall conversion efficiency of 22.5% for the OPA. With a measured signal pulse duration of 36 ps, the maximum peak power was as high as 11.1 kW. The idler had a peak power up to 4.5 kW, assuming a similar pulse width. The output parameters of this source, together with its simple fiber-laser-pumped single-pass frequency conversion configuration, makes the cascaded OP-GaAs OPG-OPA an attractive option for mid-IR spectroscopic applications.

II. Experimental Setup of OPG-OPA

The configuration of the OPG-OPA is shown in Fig. 1. The pump source was a 1952 nm diode-seeded Tm-doped-fiber MOPA system, similar to that reported in [47] and [48]. The available average output power for the OPG-OPA pump was 5.2 W, and the pulses had a duration of 46 ps at 1 MHz repetition rate. The pump had a full-width at half-maximum (FWHM) spectral bandwidth of 0.8 nm and a beam quality of $M^2 = 1.3$. In the OPG-OPA, the pump beam was divided by a polarizing beam splitter (PBS1 in Fig. 1) into two arms for launching into the OPG and OPA stages respectively. The pump power ratio between the two stages was controlled by a half-wave plate (HWP1 in Fig. 1) combined with the PBS1.

In the OPG stage, the pump was focused into an OP-GaAs crystal (BAE Systems) with a beam waist of 70 μm ($1/e^2$ radius of intensity) by an uncoated CaF_2 lens with 75-mm focal-

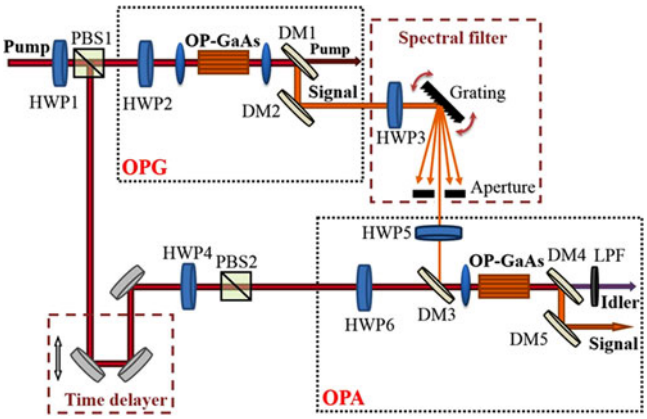

Fig. 1. Experimental setup of the OPG-OPA. HWP, half-wave plate; PBS, polarizing beam splitter; DM, dichroic mirror; LPF, long-pass filter.

length. This focusing, which is ~1.6 times bigger than confocal focusing, was chosen as a compromise between achieving the highest nonlinear gain and avoiding three-photon absorption effects [47]. The OP-GaAs crystal had five gratings with periods ranging from 57 μm to 65 μm in steps of 2 μm, and it was mounted in an oven allowing a temperature tuning range from 20 °C to 200 °C with a precision of 0.1 °C. Each grating had a dimension of 20-mm length (along the [1 $\bar{1}$ 0] crystallographic axis), 5-mm width (along [110]) and 1-mm thickness (along [001]). The pump beam propagated in the OP-GaAs along the length, which was short enough to ensure that the acceptance bandwidth (~1.4 nm) was significantly larger than the pump bandwidth (0.8 nm). Both two end facets of the OP-GaAs crystal were anti-reflection (AR) coated at the pump (R < 1%) and signal (R < 6%) wavelengths, but had a reflection of up to 17% at the longest idler wavelength (8 μm) as they had not originally been designed for operation at this wavelength. To maximize frequency conversion efficiency in the OP-GaAs, a half-wave plate (HWP2 in Fig. 1) was placed before the crystal to control the linear polarization angle. The optimum pump polarization angle was found to be at 58° with respect to [110], as reported in our recent work [47], and the generated signal polarization angle was detected to be at 10° with respect to [110]. After the crystal, an uncoated CaF_2 lens (focal length 100 mm) was used to collimate the generated signal. A pair of dichroic mirrors (DM1 and DM2 in Fig. 1), with high reflectivity at the wavelengths of signal (>95%) and high transmission at the wavelength of the pump (>90%), were used to extract the signal.

In order to convert the broad spectral output of the OPG signal generated by a particular QPM grating into a tunable narrow bandwidth seed for the OPA stage, a spectral filter consisting of a diffraction grating and a narrow aperture was used. The reflective grating (GR1325-45031, Thorlabs) with 450 grooves/mm had good diffractive efficiency (>85%), across the entire signal wavelength range generated by the OP-GaAs OPG. A half-wave plate (HWP3 in Fig. 1) was used to rotate the linear polarization angle of the output signal beam in order to optimize the grating diffraction efficiency. The adjustable-width slit aperture was placed after the grating to spatially filter the diffracted spectrum in one axis. Thus only a small but tunable fraction of the signal

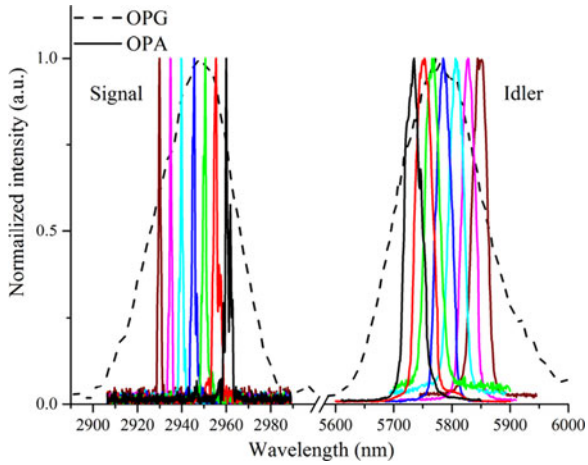

Fig. 2. Measured spectra for signal (left) and idler (right) in both OPG and OPG-OPA operation regimes based on a 57-μm QPM period grating.

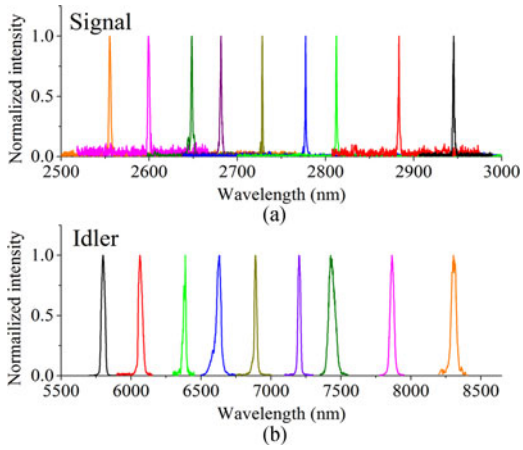

Fig. 3. Measured spectra for (a) signal and (b) idler from the tunable OPG-OPA.

generated in the OPG passed through the aperture to seed the OPA.

In the OPA stage, the temporal delay of the pump pulses reflected by the PBS1 was controlled by a pair of reflective mirrors mounted on a translation stage. A half-wave plate (HWP4 in Fig. 1) and polarizing beam splitter (PBS2 in Fig. 1) varied the pump power launched into the OP-GaAs OPA crystal, which had identical physical parameters to the OP-GaAs OPG crystal. A dichroic mirror (DM3 in Fig. 1), with coatings of high transmission (>90%) at the pump wavelengths and high reflectivity (>95%) at the signal wavelengths, spatially combined the pump and signal. The spatially and temporally overlapped beams were focused into the OP-GaAs OPA crystal, by an uncoated CaF_2 lens (focal length 100 mm), resulting in an 80 μm beam waist for the pump beam. The signal seed beam size was measured to be 85 μm when not filtered. Once the grating and slit aperture were in place the power was too low to accurately measure the beam size in the aperture axis but was estimated to be $\sim$300 μm from the geometry of the experimental setup.

III. Tuning Spectrum of OPG-OPA

For a fixed Tm-fiber MOPA wavelength of 1952nm and a fixed crystal temperature of 50 °C, the different QPM grating periods allowed tuning of the central signal and idler wavelengths of the OPG from 2588 nm to 2919 nm (signal) and from 5892 nm to 7943 nm (idler). The generated spectrum from the OP-GaAs OPG using a particular QPM grating was also relatively broad, as expected. For example, with a QPM grating period of 57 μm and temperature of 30 °C, signal at a wavelength of 2950 nm and idler at a wavelength of 5770 nm were generated from the OP-GaAs with a FWHM spectral bandwidth of 40 nm ($46\,\mathrm{cm}^{-1}$) and 170 nm ($51\,\mathrm{cm}^{-1}$), respectively, as shown in Fig. 2 (dash line).

For the OPA spectrum, taking advantage of the spectral filtering of the seed, the spectrum was substantially reduced to bandwidths of 1.2 nm ($1.4\,\mathrm{cm}^{-1}$) and 29 nm ($9\,\mathrm{cm}^{-1}$) for the signal and idler, respectively. For a fixed QPM grating period and temperature for both OP-GaAs crystals, the narrow linewidth spectrum of the OPA could be rapidly tuned across the broad OPG spectrum by rotating the diffraction grating angle, as can be found in Fig. 2 (solid line). By changing grating periods and temperatures of the two OP-GaAs simultaneously, a widely and continuously tunable OP-GaAs OPG-OPA was realized. Fig. 3 shows example output spectra, in the whole tuning range from 2552 nm to 2960 nm (signal) and from 5733 nm to 8305 nm (idler), with narrow linewidth.

IV. Output Characteristics of OPG-OPA

A pump-power threshold of approximately 1.5 W was measured for the OPG operating with signal and idler wavelengths of 2930 nm and 5860 nm, respectively (OP-GaAs period of 57 μm, oven temperature of 50 °C). The corresponding power intensity at the threshold in the OP-GaAs crystal was $212\,\mathrm{MW/cm}^2$, which is in good agreement with the predicted value of $220\,\mathrm{MW/cm}^2$ from the theory described in [49]. The measured signal and idler output powers from the OPG are shown in Fig. 4.

After a pair of dichroic mirrors (DM4, DM5 in Fig. 1) and a long-pass filter (LPF) with a short wavelength cutoff at 4.5 μm, the OPA signal and idler output power was measured. With the OPA-stage power attenuator (HWP4 + PBS2) set at a maximal transmission, the power split ratio from the PBS1 was optimized by adjusting the HWP1 to obtain the maximum signal output power from the OPA. After this optimization, we observed that 2 W of pump power was incident on the OPG crystal and 2.5 W of pump power was incident on the OPA crystal. With an OPG seed signal power of $\sim$2 mW, a maximum signal power of 400 mW, at 2942 nm, and idler power of 162 mW, at 5800 nm, were obtained for the OPA stage. The signal output power corresponded to that measured after the DMs, whereas the idler power was measured with the DMs removed but with the LPF in place and accounts for the losses of the LPF. With a 1 MHz repetition rate, the maximum pulse energies were 0.4 μJ and 0.16 μJ for the signal and idler, respectively, and the corresponding power conversion efficiency was 22.5% in the OPA stage. To investigate the influence of the pump power on the

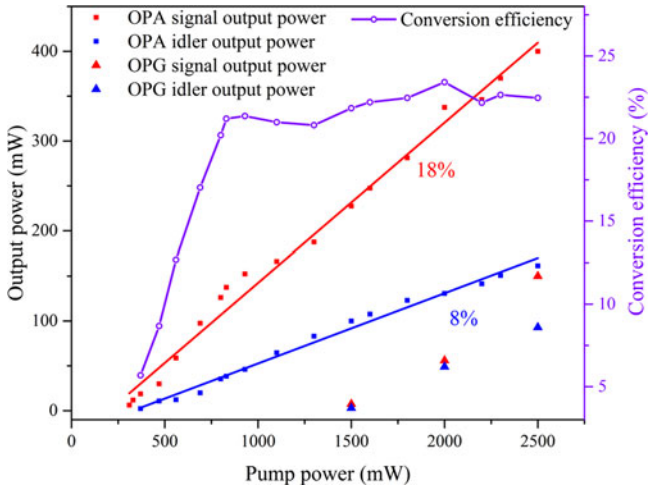

Fig. 4. (Left) Signal and idler output power as a function of pump power in OPG-OPA and OPG operation. Squares are measured OPG-OPA data points and the solid lines are linear fits. Triangles are measured OPG data points. (Right) Total power conversion efficiency of the OPG-OPA versus pump power. The solid line is purely to guide the eye.

conversion efficiency in the OPA, we measured the signal and idler output power against the pump power by adjusting the OPA power attenuator (HWP4 + PBS2), as shown in Fig. 4. The increment of the signal and idler power had a linear slope efficiency of 18% and 8%, respectively. Fig. 4 also shows the power conversion efficiency against the input pump power for the OPA. The conversion efficiency saturated when the pump was higher than ∼800 mW. The saturation at this level may be due to the non-optimized spatial overlap between the pump and the signal seed.

V. Pulse Durations and Beam Qualities

The autocorrelation (AC) traces of the pump and signal pulses, both for the OPG stage and the OPA stage, were measured with a commercial second-harmonic-generation-based autocorrelator (APE, pulseLink), as shown in Fig. 5. All AC traces have Gaussian-like pulse shapes with full width at half maximum (FWHM) values of 65 ps (pump), 51 ps (OPG signal), and 51 ps (OPG-OPA signal), respectively. The corresponding FWHM Gaussian-pulse durations were calculated to be 46 ps (pump), 36 ps (OPG signal), and 36 ps (OPG-OPA signal), respectively. In the OPG, the pulse duration of the generated signal seed was narrower than that of the pump pulse, whilst in the OPG-OPA, the pulse duration of the output signal followed that of the input signal seed, as expected. Unfortunately, the pulse duration of the idler pulses could not be measured due to the lack of suitable equipment, but the generated idler pulse durations are assumed to be similar to the generated signal pulse durations both for the OPG and OPG-OPA. Therefore, the highest peak powers can be calculated to be 11.1 kW and 4.5 kW for the cascaded OPG-OPA signal (2942 nm) and idler (5800 nm), respectively.

The M^2 parameters of the generated signal (2942 nm) and idler (5800 nm) beams from the OPG-OPA were characterized using a Pyrocam-based profiler (NanoScan, Photon). The output signal beam quality was measured to be $M_x^2 = 2.2$ and $M_y^2 = 2.4$, and the output idler beam quality was measured to be $M_x^2 = 3.4$ and $M_y^2 = 3.4$, as shown in Fig. 6.

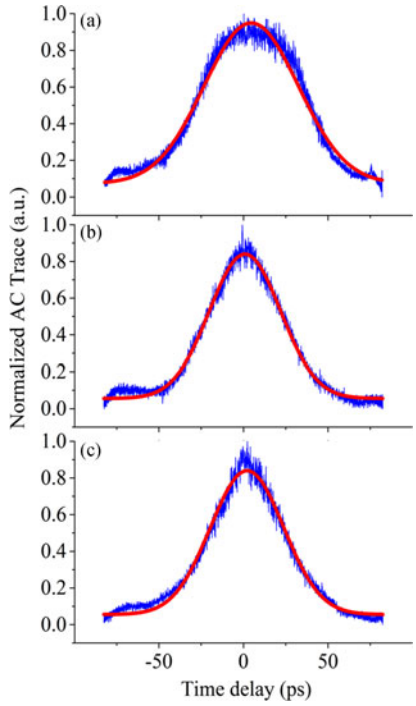

Fig. 5. Autocorrelator traces (blue) of the (a) pump pulse, (b) signal pulse of the OPG, (c) signal pulse of the OPG-OPA, and the corresponding Gaussian fits (red).

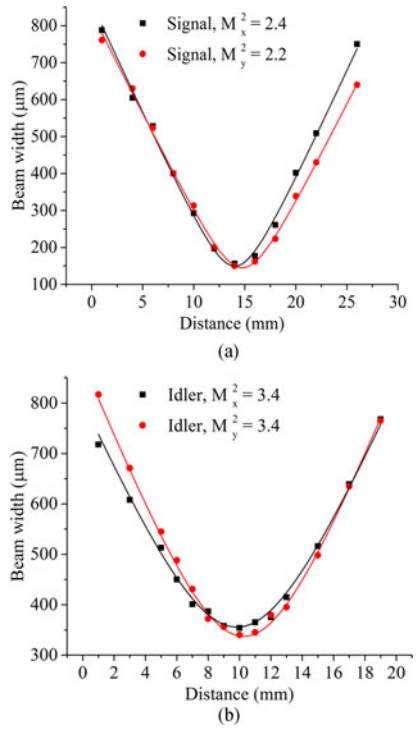

Fig. 6. M^2 measurement for (a) OPG-OPA signal at 2942 nm and (b) idler at 5800 nm in the x and y direction for OP-GaAs with grating period of 57 μm.

VI. Conclusion

In conclusion, we have demonstrated a widely tunable, narrow-linewidth, high-peak-power, cascaded picosecond optical parametric generator – optical parametric amplifier (OPG-OPA) based on OP-GaAs nonlinear crystals and a diode-seeded Tm-fibre MOPA pump laser. The OPG-OPA has generated narrow-linewidth signal and idler beams, with wavelength tuning ranges of 2552–2960 nm and 5733–8305 nm, respectively. The maximum peak powers of 11.1 kW and 4.5 kW were obtained at a signal wavelength of 2942 nm and an idler wavelength of 5800 nm with a linewidth of $1.4\,\mathrm{cm}^{-1}$ and $9\,\mathrm{cm}^{-1}$, respectively. We believe that the combination of narrow-linewidth, wide tunablity and high peak power, in a simple fibre-laser-pumped single-pass configuration, makes the cascaded OP-GaAs OPG-OPA an attractive option for mid-IR spectroscopic applications.

Acknowledgment

The data are available through the University of Southampton Research Depository (doi.org/10.5258/SOTON/D0359).

References

[1] F. K. Tittel, D. Richter, and A. Fried, "Mid-infrared laser applications in spectroscopy," in *Solid-State Mid-Infrared Laser Sources*, Berlin, Germany: Springer, 2003, pp. 458–529.

[2] G. Maisons, P. G. Carbajo, M. Carras, and D. Romanini, "Optical-feedback cavity-enhanced absorption spectroscopy with a quantum cascade laser," *Opt. Lett.*, vol. 35, no. 21, pp. 3607–3609, Nov. 2010.

[3] P. Sung Hyun, C. Jungwan, F. D. David, and K. H. Ronald, "Interference-free mid-IR laser absorption detection of methane," *Meas. Sci. Technol.*, vol. 22, no. 2, Jan. 2011, Art. no. 025303.

[4] C. S. C. Yang *et al*., "Mid-infrared, long wave infrared (4–12 μm) molecular emission signatures from pharmaceuticals using laser-induced breakdown spectroscopy," *Appl. Spectrosc.*, vol. 68, no. 2, pp. 226–231, Apr. 2014.

[5] M. W. Sigrist, "Mid-infrared laser-spectroscopic sensing of chemical species," *J. Adv. Res.*, vol. 6, no. 3, pp. 529–533, May 2015.

[6] R. Q. Yang *et al.*, "High power mid-infrared interband cascade lasers based on type-II quantum wells," *Appl. Phys. Lett.*, vol. 71, no. 17, pp. 2409–2411, Oct. 1997.

[7] R. Q. Yang, C. J. Hill, and Y. Qiu, "Mid-IR interband cascade lasers," *Proc. MRS*, vol. 891, 2006, Paper no. 0891-EE01-06.

[8] Y. Yao, A. J. Hoffman, and C. F. Gmachl, "Mid-infrared quantum cascade lasers," *Nature Photon.*, vol. 6, no. 7, pp. 432–439, Jun. 2012.

[9] M. S. Vitiello, G. Scalari, B. Williams, and P. De Natale, "Quantum cascade lasers: 20 years of challenges," *Opt. Express*, vol. 23, no. 4, pp. 5167–5182, Feb. 2015.

[10] M. Vainio and L. Halonen, "Mid-infrared optical parametric oscillators and frequency combs for molecular spectroscopy," *Phys. Chem. Chem. Phys.*, vol. 18, no. 6, pp. 4266–4294, Feb. 2016.

[11] F. Gutty *et al.*, "High peak-power laser system tuneable from 8 to 10 μm," *Adv. Opt. Technol.*, vol. 6, no. 2, pp. 95–101, Apr. 2017.

[12] M. W. Todd *et al.*, "Application of mid-infrared cavity-ringdown spectroscopy to trace explosives vapor detection using a broadly tunable (6–8 μm) optical parametric oscillator," *Appl. Phys. B*, vol. 75, no. 2, pp. 367–376, Sep. 2002.

[13] H.-S. Tan and W. S. Warren, "Mid infrared pulse shaping by optical parametric amplification and its application to optical free induction decay measurement," *Opt. Express*, vol. 11, no. 9, pp. 1021–1028, May 2003.

[14] X. Liu, R. M. Osgood, Y. A. Vlasov, and M. J. GreenWilliam, "Mid-infrared optical parametric amplifier using silicon nanophotonic waveguides," *Nature Photon.*, vol. 4, no. 8, pp. 557–560, May 2010.

[15] A. Hemming *et al.*, "99 W mid-IR operation of a ZGP OPO at 25% duty cycle," *Opt. Express*, vol. 21, no. 8, pp. 10062–10069, Apr. 2013.

[16] L. Wang *et al.*, "Mid-infrared ZGP-OPO with a high optical-to-optical conversion efficiency of 75.7%," *Opt. Express*, vol. 25, no. 4, pp. 3373–3380, Feb. 2017.

[17] S. C. Kumar *et al.*, "Compact, 1.5 mJ, 450 MHz, $CdSiP_2$ picosecond optical parametric oscillator near 6.3 μm," *Opt. Lett.*, vol. 36, no. 16, pp. 3236–3238, Aug. 2011.

[18] S. Chaitanya Kumar *et al.*, "High-power femtosecond mid-infrared optical parametric oscillator at 7 μm based on $CdSiP_2$," *Opt. Lett.*, vol. 40, no. 7, pp. 1398–1401, Apr. 2015.

[19] N. Leindecker *et al.*, "Octave-spanning ultrafast OPO with 2.6-6.1 μm instantaneous bandwidth pumped by femtosecond Tm-fiber laser," *Opt. Express*, vol. 20, no. 7, pp. 7046–7053, Mar. 2012.

[20] V. O. Smolski, S. Vasilyev, P. G. Schunemann, S. B. Mirov, and K. L. Vodopyanov, "Cr:ZnS laser-pumped subharmonic GaAs optical parametric oscillator with the spectrum spanning 3.6-5.6 μm," *Opt. Lett.*, vol. 40, no. 12, pp. 2906–2908, Jun. 2015.

[21] J. Wueppen, S. Nyga, B. Jungbluth, and D. Hoffmann, "1.95 μm-pumped OP-GaAs optical parametric oscillator with 10.6 μm idler wavelength," *Opt. Lett.*, vol. 41, no. 18, pp. 4225–4228, Sep. 2016.

[22] O. H. Heckl *et al.*, "Three-photon absorption in optical parametric oscillators based on OP-GaAs," *Opt. Lett.*, vol. 41, no. 22, pp. 5405–5408, Nov. 2016.

[23] V. O. Smolski, H. Yang, S. D. Gorelov, P. G. Schunemann, and K. L. Vodopyanov, "Coherence properties of a 2.6–7.5 μm frequency comb produced as a subharmonic of a Tm-fiber laser," *Opt. Lett.*, vol. 41, no. 7, pp. 1388–1391, Apr. 2016.

[24] P. G. Schunemann, L. A. Pomeranz, and D. J. Magarrell, "Optical parametric oscillation in quasi-phase-matched GaP," in *Proc. SPIE*, 2015, vol. 9347, Paper 93470J 7.

[25] Q. Ru, Z. Loparo, P. G. Schunemann, and K. L. Vodopyanov, "Femtosecond OPO Based on orientation-patterned gallium phosphide (OP-GaP)," in *Proc. Conf. Lasers Electro-Opt.*, San Jose, CA, USA, 2016, Paper STu1Q.6.

[26] L. A. Pomeranz *et al.*, "1-μm-pumped OPO based on orientation-patterned GaP," in *Proc. SPIE*, San Francisco, CA, USA, 2015, vol. 9347, Paper 93470K 7.

[27] T. Skauli *et al.*, "Measurement of the nonlinear coefficient of orientation-patterned GaAs and demonstration of highly efficient second-harmonic generation," *Opt. Lett.*, vol. 27, no. 8, pp. 628–630, Apr. 2002.

[28] D. French, R. Peterson, and I. Jovanovic, "Energy-scalable pulsed mid-IR source using orientation-patterned GaAs," *Opt. Lett.*, vol. 36, no. 4, pp. 496–498, Feb. 2011.

[29] P. G. Schunemann, "New nonlinear optical crystals for the mid-infrared," in *Proc. Adv. Solid State Lasers*, Berlin, Germany, 2015, Paper AM2A.2.

[30] K. Devi, P. G. Schunemann, and M. Ebrahim-Zadeh, "Continuous-wave, multimilliwatt, mid-infrared source tunable across 6.4-7.5 μm based on orientation-patterned GaAs," *Opt. Lett.*, vol. 39, no. 23, pp. 6751–6754, Dec. 2014.

[31] C. Kieleck *et al.*, "High-efficiency 20–50 kHz mid-infrared orientation-patterned GaAs optical parametric oscillator pumped by a 2 μm holmium laser," *Opt. Lett.*, vol. 34, no. 3, pp. 262–264, Feb. 2009.

[32] S. Lambert-Girard, M. Allard, M. Piché, and F. Babin, "Differential optical absorption spectroscopy lidar for mid-infrared gaseous measurements," *Appl. Opt.*, vol. 54, no. 7, pp. 1647–1656, Mar. 2015.

[33] B. Behzadi, R. Jain, and M. Hossein-Zadeh, "Narrow-linewidth mid-infrared coherent sources based on fiber-amplified Er:ZBLAN microspherical lasers," in *Conf. Laser Electro-Opt.*, San Jose, CA, USA, 2016, Paper STh1O.5.

[34] B. M. Walsh, H. R. Lee, and N. P. Barnes, "Mid infrared lasers for remote sensing applications," *J. Lumin.*, vol. 169, no. Part B, pp. 400–405, Jan. 2016.

[35] F. Kühnemann *et al.*, "Photoacoustic trace-gas detection using a CW single-frequency parametric oscillator," *Appl. Phys. B*, vol. 66, no. 6, pp. 741–745, Jun. 1998.

[36] K. L. Vodopyanov *et al.*, "$ZnGeP_2$ optical parametric oscillator with 3.8–12.4-μm tunability," *Opt. Lett.*, vol. 25, no. 11, pp. 841–843, Jun. 2000.

[37] M. Henriksson, L. Sjöqvist, V. Pasiskevicius, and F. Laurell, "Narrow linewidth 2 μm optical parametric oscillation in periodically poled $LiNbO_3$ with volume Bragg grating outcoupler," *Appl. Phys. B*, vol. 86, no. 3, pp. 497–501, Feb. 2007.

[38] S. P. Pinhas Blau, S. Fastig, and R. Lavi, "Single-mode operation of a mid-infrared optical parametric oscillator using volume-Bragg-grating cavity mirrors," *IEEE J. Quantum Electron.*, vol. 44, no. 9, pp. 867–871, Jul. 2008.

[39] K. L. Vodopyanov, I. Makasyuk, and P. G. Schunemann, "Grating tunable 4–14 μm GaAs optical parametric oscillator pumped at 3 μm," *Opt. Express*, vol. 22, no. 4, pp. 4131–4136, Feb. 2014.
[40] F. G. Colville, M. J. Padgett, and M. H. Dunn, "Continuous-wave, dual-cavity, doubly resonant, optical parametric oscillator," *Appl. Phys. Lett.*, vol. 64, no. 12, pp. 1490–1492, Mar. 1994.
[41] Q. Clément *et al.*, "Longwave infrared, single-frequency, tunable, pulsed optical parametric oscillator based on orientation-patterned GaAs for gas sensing," *Opt. Lett.*, vol. 40, no. 12, pp. 2676–2679, Jun. 2015.
[42] G. W. Baxter, Y. He, and B. J. Orr, "A pulsed optical parametric oscillator, based on periodically poled lithium niobate (PPLN), for high-resolution spectroscopy," *Appl. Phys. B*, vol. 67, no. 6, pp. 753–756, Dec. 1998.
[43] R. T. White, Y. He, B. J. Orr, M. Konno, and K. G. Baldwin, "Pulsed injection-seeded optical parametric oscillator with low frequency chirp for high-resolution spectroscopy," *Opt. Lett.*, vol. 28, no. 14, pp. 1248–1250, Jul. 2003.
[44] G. Bloom *et al.*, "Optical parametric amplification of a distributed-feedback quantum-cascade laser in orientation-patterned GaAs," *Opt. Lett.*, vol. 35, no. 4, pp. 505–507, Feb. 2010.
[45] Q. Clément *et al.*, "Tunable optical parametric amplification of a single-frequency quantum cascade laser around 8 μm in $ZnGeP_2$," *Opt. Lett.*, vol. 38, no. 20, pp. 4046–4049, Oct. 2013.
[46] F. Gutty *et al.*, "140 W peak power laser system tunable in the LWIR," *Opt. Express*, vol. 25, no. 16, pp. 18897–18906, Aug. 2017.
[47] L. Xu *et al.*, "Thulium-fiber-laser-pumped, high-peak-power, picosecond, mid-infrared orientation-patterned GaAs optical parametric generator and amplifier," *Opt. Lett.*, vol. 42, no. 19, pp. 4036–4039, Oct. 2017.
[48] S. Liang *et al.*, "High peak power picosecond pulses from an all-fiber master oscillator power amplifier seeded by a 1.95 μm gain-switched diode," in *Proc. Laser Congr.*, Nagoya, Japan, 2017, Paper ATh3A.4.
[49] P. S. Kuo *et al.*, "Optical parametric generation of a mid-infrared continuum in orientation-patterned GaAs," *Opt. Lett.*, vol. 31, no. 1, pp. 71–73, Jan. 2006.

Qiang Fu received the M.Sc. degree from Shandong University, Jinan, China. From 2016, he has been working toward the Ph.D. degree at the Optoelectronics Research Centre, University of Southampton, Southampton, U.K., working on developing novel light sources in midinfrared region. He holds a scholarship of the China Scholarship Council. His research interests include nonlinear optics and fiber amplifiers.

Lin Xu received the Ph.D. degree in optics engineering from the Shanghai Institute of Optics and Fine Mechanics, Chinese Academy of Science, Shanghai, China, in 2012. He joined the Optoelectronics Research Centre (ORC), University of Southampton as a Research Fellow in 2013. During the work in ORC, his research focuses on high peak power fiber lasers, nonlinear frequency conversions, supercontinuum generations, and midinfrared laser sources development.

Sijing Liang received the B.Sc. degree from Zhejiang University, Hangzhou, China, in 2014. Then, she joined the Optoelectronics Research Centre, University of Southampton as a Ph.D. student, studying high-power short-pulse thulium-doped fiber lasers and relevant applications. Her research interests include two-micron fiber lasers and midinfrared supercontinuum sources.

David P. Shepherd received the B.Sc. and Ph.D. degrees in physics from the University of Southampton, Southampton, U.K., in 1985 and 1989, respectively. He is currently a Professor in optoelectronics with the Optoelectronics Research Centre, University of Southampton. He is a Fellow of the Optical Society of America. His research interests include solid-state lasers and nonlinear optics, with an emphasis on ultrafast optical parametric oscillators.

David J. Richardson is currently the Deputy Director of the ORC with responsibility for fiber and laser related research. He joined the Optoelectronics Research Centre, University of Southampton as a Research Fellow in 1989 and was awarded a Royal Society University Fellowship in 1991 in recognition of his pioneering work on short-pulse fiber lasers. His research interests include optical fiber communications, microstructured optical fibers, and high-power fiber lasers. He has authored or coauthored more than 1000 conference and journal papers and holds more than 20 patents. He was one of the cofounders of SPI lasers, Ltd., and ORC spin-off venture acquired by the Trumpf Group in 2008. He is a Fellow of the Optical Society of America, the Institute of Engineering and Technology, and became a Fellow of the Royal Academy of Engineering in 2009.

Shaif-ul Alam received the B.Sc. and M.Sc. degrees in physics from the University of Dhaka, Dhaka, Bangladesh, in 1991 and 1994, respectively, and the Ph.D. degree from the Optoelectronics Research Centre, University of Southampton, Southampton, U.K., in 2000. He has more than 20 years of work experience in the field of optics at various academic and industrial positions. He was with SPI Lasers Ltd., where he was engaged in the development of numerous high-power fiber laser products. He is currently with the Optoelectronics Research Centre, University of Southampton. His research interests include the design of robust, high-power, short-pulse fiber lasers, investigation of nonlinear phenomenon in fiber and bulk materials, and nonlinear frequency conversion.